Heat and Mass Transfer 33 (1998) 443–448 © Springer-Verlag 1998

Mixed convective non-steady 3-dimensional micropolar fluid flow at a stagnation point

H. S. Takhar, R. S. Agarwal, R. Bhargava, S. Jain

Abstract The problem of mixed convective non-steady three dimensional flow of a micropolar fluid near the stagnation point of a blunt nosed body has been discussed. The governing set of differential equations are solved using the Finite Element Method. The velocity and microrotation distribution are shown graphically to depend upon four parameters namely the micropolar parameter, Grashof number, buoyancy parameter and the degree of acceleration. The conclusions are quite interesting from the application point of view.

1 Introduction

Continuum mechanical theories of the type presented by Eringen [1] which admit in addition to ordinary stresses, the presence of couple stresses, have attracted a growing interest in recent years, since they realistically describe a variety of industrial fluids such as polymers, suspension solutions, blood etc. Micropolar boundary layer flow near a stagnation point was first discussed by Williams [2], who used the Karman Polhausen integral method of solution. Peddieson and McNitt [3] applied this theory near the steady stagnation point, whereas the unsteady boundary layer flow was discussed by Kumari and Nath [4] and the 3-dimensional case was analysed by Agarwal [5].

Due to vast application, in the fields of aeronautics, chemical engineering and space research, both free and mixed convection problems have been given much consideration. Poots [6] studied laminar free convection flow near the stagnation point on a curved isothermal surface maintained at a temperature above the ambient temperature of the fluid. The steady combined forced and free convection in micropolar flow on a vertical flat plate was studied by Gorla [7].

The purpose of this paper is to examine the buoyancy effects in a forced flow in the three dimensional non-steady motion of an incompressible micropolar fluid in the vicinity of the forward stagnation point of a blunt nosed body. The prediction of heat transfer characteristics encompasses a wide range of technological applications, such as cooling in aerofoils, fibre spinning etc. The velocity of the potential flow is chosen to vary inversely as a linear function of time. Four parameters viz. R, the micropolar parameter, G, the Grashof number, (a measure of buoyancy), C, the parameter characterising the surface around the stagnation point and D, the degree of deceleration of the potential flow, govern the flow phenomenon. The differential equations are solved by the finite element method and the results are shown graphically. These results are also compared with the corresponding flow problem in the viscous case and found to be in satisfactory agreement.

Received on 4 June 1997

H. S. Takhar
Manchester School of Engineering, University of Manchester
Manchester, M13 9PL, U.K.

R. S. Agarwal, R. Bhargava, S. Jain
Department of Mathematics, University of Roorkee
Roorkee-247667, India

Correspondence to: H. S. Takhar

2 Mathematical formulation

Consider an unsteady, laminar combined convective flow at a three-dimensional stagnation point $(x = y = z = 0)$ on a blunt nosed body, which is not necessarily axially symmetric. The forced flow, which approaches the body in the negative z-direction impinges on the surface normally at the stagnation point, flowing away radially in all directions along the surface and is assumed to have unsteady velocity components U and V in x and y directions respectively. The free stream temperature is taken as constant and the dissipation effects near the stagnation point are assumed to be negligible. The fluid has constant properties except the density variation (due to temperature difference) which is used to express the body force term as a buoyancy term. The governing equations are given by

$$\frac{\partial u}{\partial x}+\frac{\partial v}{\partial y}+\frac{\partial w}{\partial z}=0 \tag{1}$$

$$\frac{\partial u}{\partial t}+u\frac{\partial u}{\partial x}+v\frac{\partial u}{\partial y}+w\frac{\partial u}{\partial z}=-\frac{\partial p}{\partial x}-f_x + \frac{(\mu+k)}{\rho}\left[\frac{\partial^2 u}{\partial x^2}+\frac{\partial^2 u}{\partial y^2}+\frac{\partial^2 u}{\partial z^2}\right]-\frac{k}{\rho}\left[\frac{\partial v_2}{\mathrm{d}z}-\frac{\partial v_3}{\partial y}\right] \tag{2}$$

$$\frac{\partial v}{\partial t}+u\frac{\partial v}{\partial x}+v\frac{\partial v}{\partial y}+w\frac{\partial v}{\partial z}=-\frac{\partial p}{\partial y}-f_y + \frac{(\mu+k)}{\rho}\left[\frac{\partial^2 v}{\partial x^2}+\frac{\partial^2 v}{\partial y^2}+\frac{\partial^2 v}{\partial z^2}\right]-\frac{k}{\rho}\left[\frac{\partial v_3}{\partial x}-\frac{\partial v_1}{\partial z}\right] \tag{3}$$

$$\frac{\partial w}{\partial t}+u\frac{\partial w}{\partial x}+v\frac{\partial w}{\partial y}+w\frac{\partial w}{\partial z}=-\frac{\partial p}{\partial z}-f_z$$
$$+\frac{(\mu+k)}{\rho}\left[\frac{\partial^2 w}{\partial x^2}+\frac{\partial^2 w}{\partial y^2}+\frac{\partial^2 w}{\partial z^2}\right]-\frac{k}{\rho}\left[\frac{\partial v_1}{\partial y}-\frac{\partial v_2}{\partial x}\right] \quad (4)$$

$$\rho j\left(\frac{\partial v_1}{\partial t}+u\frac{\partial v_1}{\partial x}+v\frac{\partial v_1}{\partial y}+w\frac{\partial v_1}{\partial z}\right)=(\alpha+\beta+\gamma)$$
$$\times\frac{\partial}{\partial x}\left(\frac{\partial v_1}{\partial x}+\frac{\partial v_2}{\partial y}+\frac{\partial v_3}{\partial z}\right)-\gamma\frac{\partial}{\partial y}\left(\frac{\partial v_2}{\partial x}-\frac{\partial v_1}{\partial y}\right)$$
$$-\gamma\frac{\partial}{\partial z}\left(\frac{\partial v_3}{\partial x}-\frac{\partial v_1}{\partial z}\right)-k\left(\frac{\partial v}{\partial z}-\frac{\partial w}{\partial y}\right)-2kv_1 \quad (5)$$

$$\rho j\left[\frac{\partial v_2}{\partial t}+u\frac{\partial v_2}{\partial x}+v\frac{\partial v_2}{\partial y}+w\frac{\partial v_2}{\partial z}\right]=(\alpha+\beta+\gamma)$$
$$\times\frac{\partial}{\partial y}\left[\frac{\partial v_1}{\partial x}+\frac{\partial v_2}{\partial y}+\frac{\partial v_3}{\partial z}\right]-\gamma\frac{\partial}{\partial z}\left[\frac{\partial v_3}{\partial y}-\frac{\partial v_2}{\partial x}\right]$$
$$-\gamma\frac{\partial}{\partial x}\left[\frac{\partial v_1}{\partial y}-\frac{\partial v_2}{\partial x}\right]-k\left[\frac{\partial w}{\partial x}-\frac{\partial u}{\partial z}\right]-2kv_2 \quad (6)$$

$$\rho j\left[\frac{\partial v_3}{\partial t}+u\frac{\partial v_3}{\partial x}+v\frac{\partial v_3}{\partial y}+w\frac{\partial v_3}{\partial z}\right]=(\alpha+\beta+\gamma)$$
$$\times\frac{\partial}{\partial z}\left[\frac{\partial v_1}{\partial x}+\frac{\partial v_2}{\partial y}+\frac{\partial v_3}{\partial z}\right]-\gamma\frac{\partial}{\partial x}\left[\frac{\partial v_1}{\partial z}-\frac{\partial v_3}{\partial x}\right]$$
$$-\gamma\frac{\partial}{\partial y}\left[\frac{\partial v_2}{\partial z}-\frac{\partial v_3}{\partial y}\right]-k\left[\frac{\partial u}{\partial y}-\frac{\partial v}{\partial x}\right]-2kv_3 \quad (7)$$

$$c_p\left[\frac{\partial T}{\partial t}+u\frac{\partial T}{\partial x}+v\frac{\partial T}{\partial y}+w\frac{\partial T}{\partial z}\right]$$
$$=K_f\left[\frac{\partial^2 T}{\partial x^2}+\frac{\partial^2 T}{\partial y^2}+\frac{\partial^2 T}{\partial z^2}\right] . \quad (8)$$

The boundary conditions on velocity and temperature are taken as

$$u=0,\quad v=0,\quad w=0,\quad T=T_w,\quad \text{at}\quad z=0$$
$$u\to U,\quad v\to V,\quad T\to T_\infty,\quad \text{as}\quad z\to\infty \quad (9a)$$

For microrotation, the following two types of boundary conditions are assumed:

$$\text{Case (i): } v_1=-\frac{1}{2}\frac{\partial v}{\partial z},\quad v_2=\frac{1}{2}\frac{\partial u}{\partial z},\quad v_3=0,\quad \text{at}\quad z=0$$
$$v_1\to 0,\quad v_2\to 0,\quad v_3\to 0,\quad \text{as}\quad z\to\infty \quad (9b)$$

where v_1 and v_2 are taken to be equal to the angular velocities at the surface, i.e. the antisymmetric part of stress vanishes at the surface.

$$\text{Case (ii): } v_1=v_2=v_3=0,\quad \text{at}\quad z=0$$
$$v_1\to 0,\quad v_2\to 0,\quad v_3\to 0,\quad \text{as}\quad z\to\infty \quad (9c)$$

which define the no spin boundary conditions on the surface.

Following Cheng [8], U and V are chosen as

$$U=\frac{Ax}{(1+\varepsilon t)}\quad\text{and}\quad V=\frac{By}{(1+\varepsilon t)} .$$

Accordingly, the z-direction velocity component W, of the potential flow shall be

$$W=\frac{(A+B)z}{(1+\varepsilon t)}$$

where A, B and ε are constants. Without loss of generality, we choose the x-axis such that $A>0$, B may be positive or negative such that $(A+B)>0$, in order to ensure the third component to be in the negative z-direction. The non-dimensional forms for various quantities may be taken as

$$\eta=\left[\frac{A\rho}{\mu(1+\varepsilon t)}\right]^{1/2}z,\quad u=\frac{Ax}{(1+\varepsilon t)}f'(\eta),$$
$$v=\frac{By}{(1+\varepsilon t)}g'(\eta),\ w=-\left[\frac{A\rho}{\mu(1+\varepsilon t)}\right]^{1/2}(Af+Bg),$$
$$v_1=\frac{By}{(1+\varepsilon t)^{3/2}}\left[\frac{A\rho}{\mu}\right]^{1/2}\phi_1(\eta),$$
$$v_2=\frac{Ax}{(1+\varepsilon t)^{3/2}}\left[\frac{A\rho}{\mu}\right]^{1/2}\phi_2(\eta),$$
$$v_3=\frac{A+B}{2(1+\varepsilon t)}\phi_3(\eta),\ \frac{T-T_\infty}{T_w-T_\infty}=\frac{ABL^4\rho^2}{(1+\varepsilon t)^2\mu^2}\theta(\eta) \quad (10)$$

and for pressure, the following expression has been taken

$$P_s-P=\frac{A^2\rho}{2(1+\varepsilon t)^2}\left[(1-D)x^2+C^2\left(1-\frac{D}{C}\right)y^2\right.$$
$$+\left(1+2C+C^2\right)\left(1+\frac{D}{1+C}\right)F(\eta)$$
$$\left.+\frac{\mu}{\rho}\left(\frac{1}{A}+Dt\right)\right] \quad (11)$$

where $C(=B/A)$ is the parameter characterising the surface around the stagnation point and $D(=\varepsilon/A)$ is the degree of acceleration or deceleration of the potential flow.

As in [6], expressing the body force, due to density variation as a result of temperature difference, by

$$-\frac{\partial p_s}{\partial x}-\rho f_x=\rho_\infty g_e\beta_1(T-T_\infty)x \quad (12a)$$
$$-\frac{\partial p_s}{\partial y}-\rho f_y=\rho_\infty g_e\beta_1(T-T_\infty)y \quad (12b)$$
$$-\frac{\partial p_s}{\partial z}-\rho f_z=\rho_\infty g_e\beta_1(T-T_\infty)z \quad (12c)$$

where g_e is the gravitational force.
Equations (1–8) may be written as

$$(1+R)f'''+(f+Cg)f''-f'^2-D\left(1-f'-\frac{\eta}{2}f''\right)$$
$$-R\phi_2'+CG\theta+1=0 \quad (13)$$
$$(1+R)g'''+(f+Cg)g''-Cg'^2-D\left(1-g'-\frac{\eta}{2}g''\right)$$
$$+R\phi_1'+C+G\theta=0 \quad (14)$$

$$(1+R)(f''+Cg'')+ff'+Cf'^{g}+Cf'^{g}+C^2gg' + \tfrac{D}{2}(\eta f'+C\eta g'+f+Cg) \quad (15)$$

$$-\tfrac{1}{2}(1+2C+C^2+D+CD)f'+R(C\phi_1-\phi_2) - C\eta G\theta = 0$$

$$R_1C\phi_1''+(f+Cg)C\phi_1'-C^2g'\phi_1+D\left(\tfrac{3}{2}C\phi_1+C\tfrac{\eta}{2}\phi_1'\right) - RR_2(Cg''+2C\phi_1)=0 \quad (16)$$

$$R_1\phi_2''+(f+Cg)\phi_2'-f'\phi_2+\tfrac{D}{2}\left(3\phi_2+\eta\phi_2'\right) + RR_2(f''-2\phi_2)=0 \quad (17)$$

$$R_3\phi_3''+(f+Cg)\phi_3'+\frac{D\eta}{2}\phi_3'+D\phi_3-2R_2\phi_3=0 \quad (18)$$

$$\theta''+\Pr\left[(f+Cg)\theta'+\tfrac{D}{2}\eta\theta'+2D\theta\right]=0 \quad (19)$$

where,

$$R=\frac{k}{\mu},\quad R_1=\frac{\gamma}{\mu j},\quad R_2=\frac{\mu L}{Uj\rho},\quad R_3=\frac{\alpha+\beta+\gamma}{\mu j},$$

$$\Pr=\frac{\mu C_p}{K_f},\quad G=\frac{g_e\beta_1(T_w-T_\infty)L^3\rho^2}{\mu^2}\ .$$

where R is the micropolar parameter and G is the Grashof number, Pr is the Prandtl number, and the remainder are micropolar constants.

The boundary conditions (9) reduce to

$$f=g=0,\quad f'=g'=0,\quad \theta=1,\quad \text{at}\quad \eta=0$$
$$f'\to 1,\quad g'\to 1,\quad \theta\to 0,\quad \text{as}\quad \eta\to\infty \quad (20a)$$

$$\text{Case (i): } \phi_1=\tfrac{1}{2}g''(0),\ \phi_2=-\tfrac{1}{2}f''(0),\ \phi_3=0,\ \text{at } \eta=0$$
$$\phi_1\to 0\quad \phi_2\to 0\quad \phi_3\to 0,\quad \text{as}\quad \eta\to\infty \quad (20b)$$

$$\text{Case (ii): } \phi_1=0,\quad \phi_2=0,\quad \phi_3=0,\quad \text{at}\quad \eta=0$$
$$\phi_1\to 0,\quad \phi_2\to 0,\quad \phi_3\to 0,\quad \text{as}\quad \eta\to\infty\ . \quad (20c)$$

From Eq. (18) and the corresponding boundary conditions, it is clear that the microrotation component ϕ_3 does not exist. It is to be noted that Eqs. (13–14), (16–17) and (19) are coupled while Eq. (15) is independent and it can be directly integrated after evaluating the functions f, g, ϕ_1, ϕ_2, θ and their derivatives.

2.1 Method of solution

To solve the set of non linear differential equations (13, 14, 16, 17, and 19) subject to boundary conditions (20), the finite element method as given by Reddy [9] has been applied. Following this, the equations and boundary conditions may be written as

$$f'-h=0 \quad (21)$$

$$(1+R)h''+\tfrac{D\eta}{2}h'+Dh-h^2+(f+Cg)h' + CG\theta-R\phi_2'=(D-1) \quad (22)$$

$$g'-s=0 \quad (23)$$

$$(1+R)s''+\tfrac{D\eta}{2}s'-Cs^2+(f+Cg)s' + G\theta+R\phi_1'=(D-C) \quad (24)$$

$$R_1\phi_1''+(f+Cg)\phi_1'-Cs\phi_1+D\left(\tfrac{3}{2}\phi_1+\tfrac{\eta}{2}\phi_1'\right) - RR_2(s'+2\phi_1)=0 \quad (25)$$

$$R_1\phi_2''+(f+Cg)\phi_2'-h\phi_2+D\left(\tfrac{3}{2}\phi_1+\tfrac{\eta}{2}\phi_1'\right) + RR_2(h'-2\phi_2)=0 \quad (26)$$

$$\theta''+\Pr\left[(f+Cg)\theta'+\tfrac{D}{2}\eta\theta'+2D\theta\right]=0 \quad (27)$$

$$f(0)=0,\quad h(0)=0,\quad g(0)=0,\quad s(0)=0,\quad \theta(0)=1$$
$$h(\infty)=1,\quad s(\infty)=1,\quad \theta(\infty)=0 \quad (28a)$$

and

$$\text{Case (i): } \phi_1(0)=\tfrac{1}{2}s'(0),\quad \phi_2(0)=\tfrac{1}{2}h'(0),\quad \phi_3(0)=0$$
$$\phi_1(\infty)=0,\quad \phi_2(\infty)=0,\quad \phi_3(\infty)=0 \quad (28b)$$

$$\text{Case (ii): } \phi_1(0)=0,\quad \phi_2(0)=0,\quad \phi_3(0)=0$$
$$\phi_1(\infty)=0,\quad \phi_2(\infty)=0,\quad \phi_3(\infty)=0\ . \quad (28c)$$

For computational purposes the ∞ is taken at $\eta=8$ and the domain is divided into a set of line elements say $(N=40)$. The variational form associated with the Eqs. (21–27) over a typical element $(\eta_e+\eta_{e+\eta})$ is given by

$$\int_{\eta_e}^{\eta_{e+1}} w_1(f'-h)\,d\eta=0$$

$$\int_{\eta_e}^{\eta_{e+1}} w_2\left[(1+R)h''+\frac{D\eta}{2}h'+Dh-h^2+(f+Cg)h' + CG\theta-R\phi_2'-(D-1)\right]d\eta=0$$

$$\int_{\eta_e}^{\eta_{e+1}} w_3(g'-s)\,d\eta=0$$

$$\int_{\eta_e}^{\eta_{e+1}} w_4\left[(1+R)s''+\frac{D\eta}{2}s'-Cs^2+(f+Cg)s' + G\theta+R\phi_1'-(D-C)\right]d\eta=0$$

$$\int_{\eta_e}^{\eta_{e+1}} w_5\left[R_1\phi_1''+(f+Cg)\phi_1'-Cs\phi_1+D\left(\tfrac{3}{2}\phi_1+\tfrac{\eta}{2}\phi_1'\right) - RR_2(s'+2\phi_1)\right]d\eta=0$$

$$\int_{\eta_e}^{\eta_{e+1}} w_6\left[R_1\phi_2''+(f+Cg)\phi_2-h\phi_2+D\left(\tfrac{3}{2}\phi_1+\tfrac{\eta}{2}\phi_1'\right) + RR_2(h'-2\phi_2)\right]d\eta=0$$

$$\int_{\eta_e}^{\eta_{e+1}} w_7\left[\theta''+\Pr\left[(f+Cg)\theta'+\tfrac{D}{2}\eta\theta'+2D\theta\right]\right]d\eta=0$$

where $w_j, j = (1,7)$ are arbitrary test functions and may be viewed as the variation in f, g, h, s, ϕ_1, ϕ_2 and θ respectively. The finite element approximations are taken in the form

$$f = \sum_{j=1}^{2} f_j \psi_j,\ h = \sum_{j=1}^{2} h_j \psi_j,\ g = \sum_{j=1}^{2} g_j \psi_j,\ s = \sum_{j=1}^{2} s_j \psi_j\ ,$$

$$\phi_1 = \sum_{j=1}^{2} \phi_{1j} \psi_j,\ \phi_2 = \sum_{j=1}^{2} \phi_{2j} \psi_j,\ \theta = \sum_{j=1}^{2} \theta_j \psi_j$$

and

$$w_1 = w_2 = w_3 = w_4 = w_5 = w_6 = w_7 = \psi_i \quad (i = 1,2)\ .$$

Then the finite element model of equations in accordance with Reddy [9] may be written as:

$$\left[K^{ij}\right]\left[F_j\right] = \left[R_i\right]$$

where $\left[K^{ij}\right]$ is the stiffness matrix. F_j are the column vectors of known functions. The global matrix is obtained through the assembly of element equations and are solved for velocity, microrotation and temperature. The details can be seen from Reddy [9]. The system of equations, so obtained, is non-linear and is solved using the Newton linearization process.

3
Numerical results and discussion

The numerical results for the velocity, microrotation and temperature functions are obtained correct to six decimal places for different values of C, the parameter characterising the surface around the stagnation point. D the degree of acceleration, R the micropolar parameter and G the Grashof number.

The results for the velocity, microrotation and temperature for $C = 0.5$ only ($C < 0$ corresponds to saddle point of attachment and $C > 0$ to the nodal point of attachment) have been shown graphically due to the symmetric nature of the velocity profiles. The parameter $D = 0$ (i.e. $\varepsilon = 0$) gives the steady state flow, the case $D < 0$ (i.e. $\varepsilon < 0$) corresponds to the acceleration flow while $D > 0$ (i.e. $\varepsilon > 0$) to the deceleration flow. However, the range of D from -1.0 to 1.0 covers most practical cases of accelerating or decelerating flow. The value of the micropolar parameter $R = 0$ corresponds to the viscous case while $\mathrm{Gr} = 0$ gives the pure forced convective flow, the numerical results for $\mathrm{Gr} = 0$ are similar to Agarwal [5]. Also it has been noticed that the velocity variations with the change in R_1 and R_2 are not appreciable and as such they are fixed for 1.5 and 1.0 respectively.

Figures 1 and 2 show the velocity profile for various values of R, Gr and D. From Fig. 1, it is clear that the boundary layer thickness increases as R increases for both accelerating ($D < 0$) and decelerating ($D > 0$) flow. The situation is reversed with an increase in Gr for a fixed $R = 5$ (Fig. 2). The change in velocity is not very significant for change in D.

Figures 3 and 4 show the microrotation distribution for various values of R, G and D respectively. These show that the angular velocity is maximum at the surface which

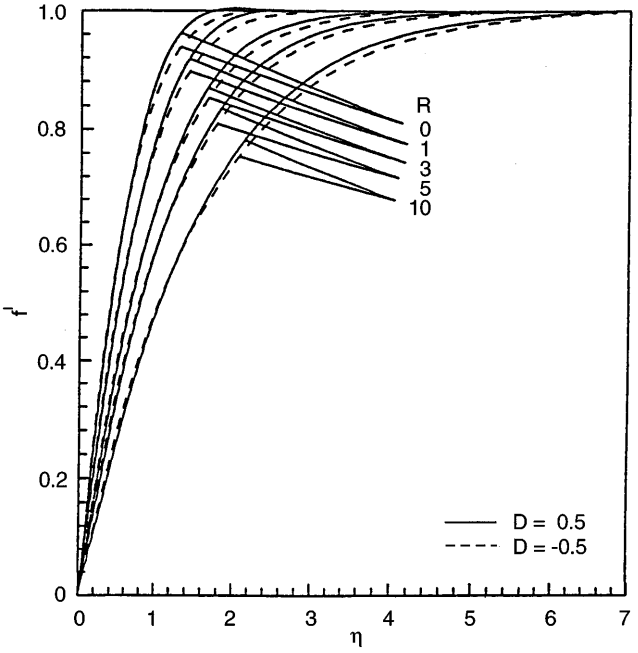

Fig. 1. Velocity distribution for various values of R ($C = 0.5,\ G = 1.0$)

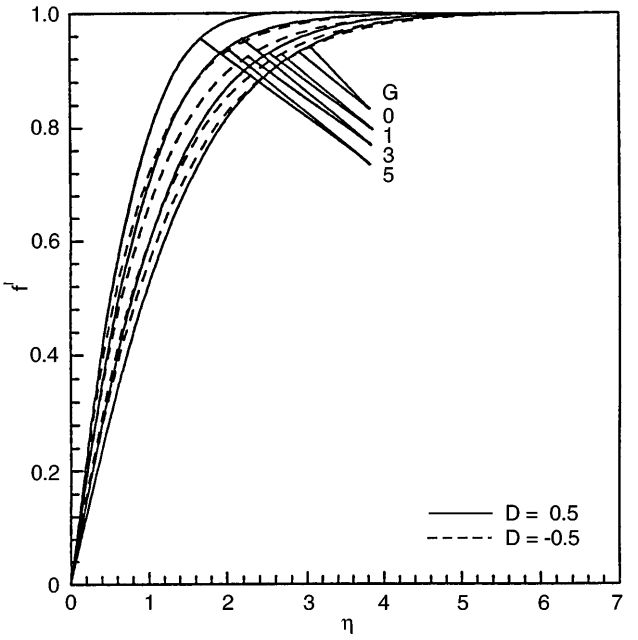

Fig. 2. Velocity distribution for various values of G ($R = 1.0,\ C = 0.5$)

decreases monotonically. The microrotation decreases near the surface but increases after a finite distance on increasing R for both $D > 0$ and $D < 0$. Figure 4 depicts that the microrotation increases near the surface but decreases as one moves away from the surface with an increase in Grashof number. A similar behaviour is observed for decelerating and steady flow.

In Figs. 5 and 6 the temperature distribution is shown. It is evident that the surface cools down as the temperature decreases monotonically for accelerating flow ($D < 0$),

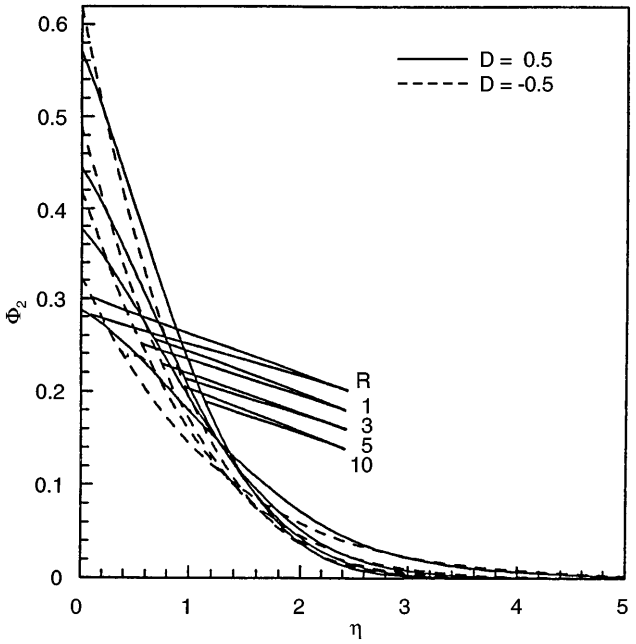

Fig. 3. Microrotation distribution for various values of R ($C = 0.5$, Gr $= 1.0$)

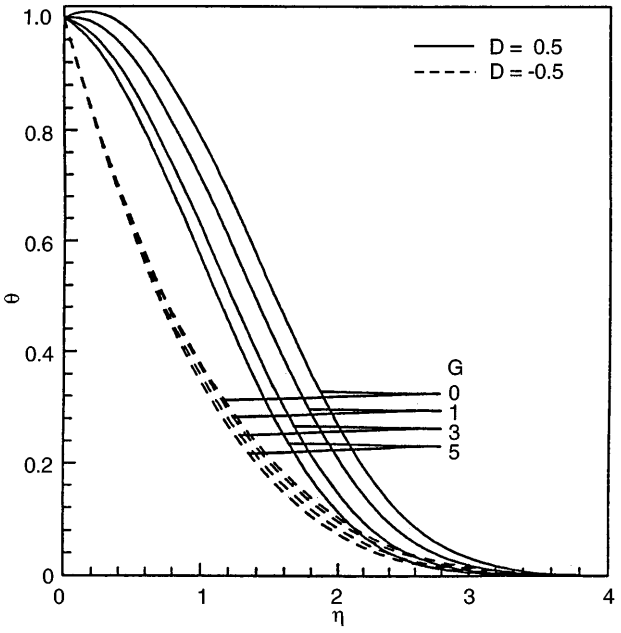

Fig. 5. Temperature distribution for various values of R ($C = 0.5$, Gr $= 1.0$)

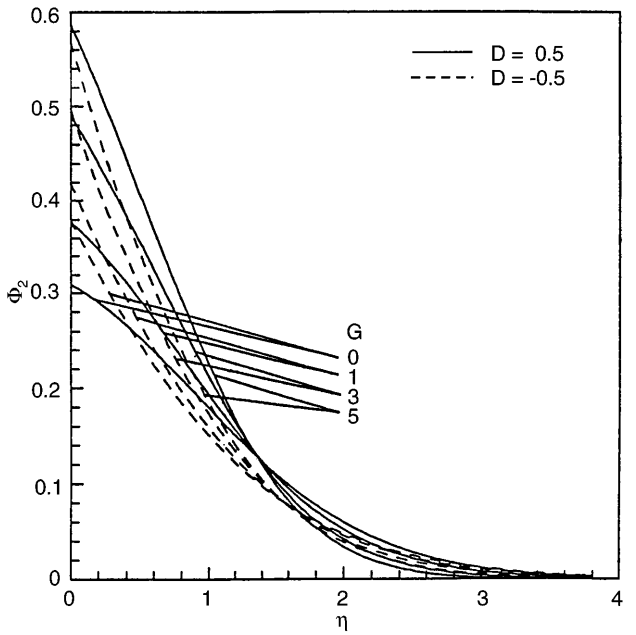

Fig. 4. Microrotation distribution for various values of G ($R = 1.0$, $C = 0.5$)

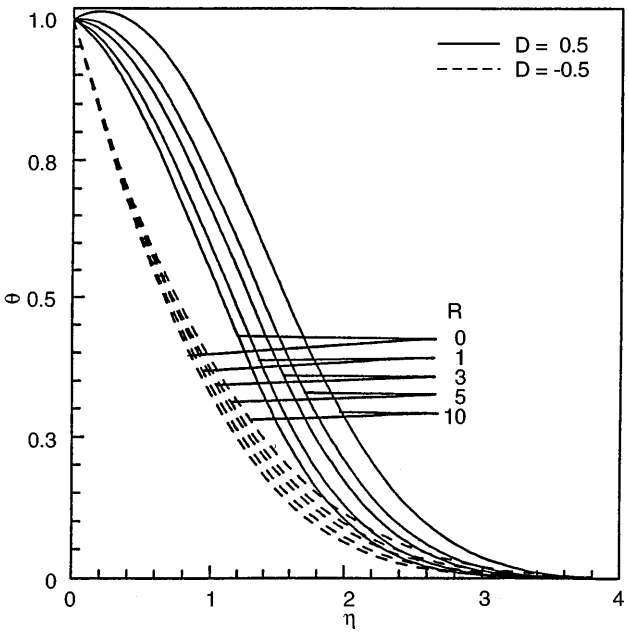

Fig. 6. Temperature distribution for various values of G ($R = 1.0$, $C = 0.5$)

while there is slight increase in temperature near the surface for decelerating flow. Figure 5 shows that the cooling takes place slowly as R increases however, the temperature decreases sharply with an increase in buoyancy parameter G (Fig. 6). It is also observed that for decelerating flow the temperature near the surface exceeds the surface temperature which implies that heat is being transferred from the fluid to the surface and therefore the surface will be heated instead of being cooled which may be useful in practice.

The numerical values of the skin friction coefficients $f''(0)$ and $g''(0)$ for x and y direction are tabulated in Table 1. It shows that the micropolar fluid reduces the skin friction coefficient as compared to the Newtonian fluid ($R = 0$), but the skin friction coefficient increases as the buoyancy force increases. For $D < 0$, the skin friction is more while the reverse happens for $D > 0$ as compared to the steady case. The nature of couple stress coefficients with varying D is the same as that of the skin friction coefficients.

In contrast to the skin friction and the couple stress, the heat transfer is strongly affected by D for all values of R and G. It is observed from Table 2 that the heat transfer parameter $\theta'(0)$ decreases as R increases while the reverse

Table 1. Numerical values of the skin-friction coefficients for the x and y directions $C = 0.5$

	$D = -0.5$		$D = 0.0$		$D = 0.5$	
	$f''(0)$	$g''(0)$	$f''(0)$	$g''(0)$	$f''(0)$	$g''(0)$
$R = 0$, $G = 0$	1.2915	1.0833	1.1957	0.9640	1.0904	0.8304
$R = 1$, $G = 1$	1.2375	1.2322	1.1835	1.1989	1.1420	1.1983
$R = 3$, $G = 1$	0.9783	0.9508	0.9289	0.9139	0.8896	0.9053
$R = 3$, $G = 3$	1.1741	1.3513	1.1590	1.3881	1.1677	1.4781

Table 2. Numerical values of the heat transfer coefficients $C = 0.5$

	$D = -0.5$	$D = 0.0$	$D = 0.5$
	$-\theta'(0)$	$-\theta'(0)$	$-\theta'(0)$
$R = 0$, $G = 0$	0.9390	0.5882	0.0900
$R = 1$, $G = 1$	0.9364	0.5905	0.1167
$R = 3$, $G = 1$	0.9151	0.5521	0.0309
$R = 3$, $G = 3$	0.9340	0.5931	0.1403

happens as G increases. From the analysis, it may be inferred that the presence of micropolar additives thoroughly influences the characteristic features of the flow and heat transfer. The heat transfer and skin friction are found to decrease as the micropolar parameter increases. In a nuclear reactor, considerable reduction in heat transfer is needed. The present analysis could be of help in choosing a micropolar fluid with appropriate combination of material particles so that the reduction in heat transfer and drag may be achieved accordingly.

References

1. **Eringen AC** (1966) Theory of micropolar fluids. J Math Mech 16: 1–18
2. **Williams JC III** (1968) Non-steady stagnation point flow. AIAA J 6: 2417–2419
3. **Peddieson J; McNitt RP** (1970) Boundary layer theory for a micropolar fluid. Recent Adv Engng Sci 5: 405–476
4. **Kumari M; Nath G** (1988) Unsteady incompressible boundary layer flow of micropolar fluid at a stagnation point. Int J Engng Sci 22: 755–767
5. **Agarwal RS; Bhargava R; Balaji AVS** (1990) Finite element solution of non-steady three dimensional micropolar fluid flow at a stagnation point. Int J Engng Sci 28: 851–857
6. **Poots G** (1964) Laminar free convection near the lower stagnation point on an isothermal curved surface. Int J Heat Mass Trans 7: 863–874
7. **Gorla RSR** (1988) Combined forced and free convection in micropolar boundary layer flow on a vertical flat plate. Int J Engng Sci 26: 385–391
8. **Cheung EHW; Ozisik MN; Williams JC III** (1971) Non-steady three dimensional stagnation point flow. Trans ASME J Appl Mech 38: 282–287
9. **Reddy JN** (1985) An introduction to the finite element method. McGraw Hill Book Company, New York